Confinement properties of a low-beta discharge in a spindle cusp magnetic field

Robert A. Bosch and Robert L. Merlino
Department of Physics and Astronomy, The University of Iowa, Iowa City, Iowa 52242

(Received 2 December 1985; accepted 11 March 1986)

An experimental study of the confinement properties of a low-(average) beta discharge plasma in a spindle cusp magnetic field is described. Electron and ion densities, space potentials, and plasma flow velocities were measured in the ring and point cusps. The leak width of the escaping plasma was measured over a large range of magnetic field strengths and neutral pressures. Leak widths varying between the hybrid gyrodiameter and the ion gyrodiameter were observed. The dependence of the leak width on neutral pressure and magnetic field is accounted for by a simple model in which plasma diffuses across the magnetic field as a result of neutral particle collisions while streaming out of the cusps along the magnetic field lines. At the lowest neutral pressures investigated, the scaling of the leak width with magnetic field strength suggests that noncollisional mechanisms (e.g., Bohm diffusion) determine the leak width.

I. INTRODUCTION

Magnetic field geometries containing cusps are widely used in laboratory devices for basic plasma physics studies. These low-temperature discharge devices employing multipolar cusp confinement have been studied since 1973, when Limpaecher and MacKenzie[1] showed that they could be used to confine large-volume, uniform, quiescent plasmas with densities 100 times larger than in double-plasma devices[2] without surface cusp magnetic fields.

Although magnetic cusps were initially investigated as possible thermonuclear fusion plasma confinement schemes,[3,4] their continued use has been in devices for basic plasma studies and in various applied areas, e.g., in ion-beam sources.[5] Multipolar confinement is also being actively investigated for use in plasma-etching reactors.[6] The efficiency of such devices depends directly on plasma losses through the cusps.

Of particular interest are the profiles of plasma escaping through the cusps (characterized by the full width at half-maximum—the so-called cusp leak width), the plasma flow velocity in the cusps, and the electrostatic potentials in the cusps. In low-beta discharge plasmas operated at sufficiently low neutral pressures, leak widths of order $2(r_{ce}r_{ci})^{1/2}$ (the hybrid gyrodiameter) have been reported,[3,7-9] although under different conditions leak widths of order r_{ci} have also been observed.[10,11] Hershkowitz *et al.*[7] found that the leak width scaled as $m_i^{1/4}B^{-1}$ when the magnetic field was varied by a factor of 2 for three different ion masses at a fixed pressure. Measurements of the plasma space potential in the cusps[11,12] indicated the presence of electrostatic fields, which impede the cross-field motion of ions (resulting in narrow ion leak widths) while accelerating the ions out of the cusps along the magnetic field lines.

Many aspects of the experimental results are not yet fully understood, and numerous explanations for the cusp leak width have been proposed. These include considerations of electrostatic effects[3,4,13,14] collisions,[3,4,13,15,16] and turbulence.[3,4,8,17]

This paper describes an experimental investigation of the confinement of an argon discharge plasma in a magnetic spindle cusp. The plasma density, potential profiles, and velocity of the escaping plasma were measured in both the ring and point cusps. The dependence of the electron and ion leak widths on plasma density was determined over a wide range of densities. At densities sufficiently high that the plasma in the cusp was quasineutral, it was observed that the ion leak width was reduced, presumably as a result of self-consistent electric fields. The leak width measurements were also made over a large range of magnetic field and neutral pressure so that their scaling could be determined. The observed scalings are accounted for in terms of a simple analytic model in which the plasma diffuses across the magnetic field while streaming out along the magnetic field.

The apparatus and experimental techniques are described in Sec. II. In Sec. III we present the experimental results, which are then discussed in Sec. IV. The results and conclusions are summarized in Sec. V.

II. EXPERIMENTAL APPARATUS

The experimental apparatus is shown in Fig. 1. A cylindrical stainless steel chamber, 90 cm in length and 60 cm in diameter, was evacuated to a base pressure of $\sim 5\times 10^{-7}$ Torr. The chamber contained two water-cooled coils of 17 cm inner diameter that produced a spindle cusp magnetic field using currents of up to 1000 A. Each coil was made of six turns of 6.35 mm ($\frac{1}{4}$ in.) copper tubing in a teflon insulating sleeve enclosed in an aluminum shell that was connected electrically to the grounded chamber. The maximum magnetic field in the center of the ring cusp was 160 G, while the maximum field in the center of the point cusp was 260 G.

In the center of the chamber, up to 24 (12, typically) thoriated tungsten filaments of 0.13 mm diameter and 2 cm length were mounted between two 16 mm diam copper disks. Current was passed through a copper rod to one of the disks, from which it returned coaxially through the filaments, the other disk, and 6.35 mm ($\frac{1}{4}$ in.) copper tubing.

 0031-9171/86/061998-09$01.90

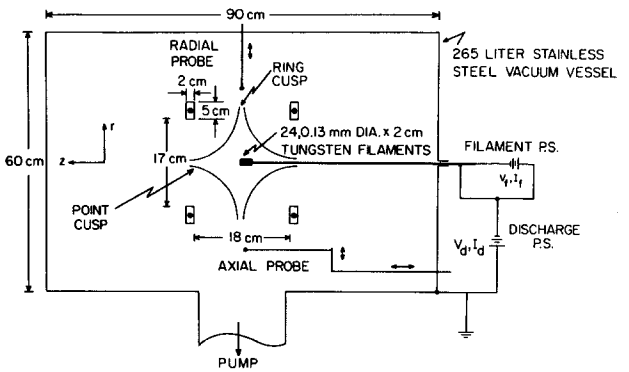

FIG. 1. Schematic diagram of spindle cusp device. Measurements could be made with the filament structure entering through either the ring or point cusps.

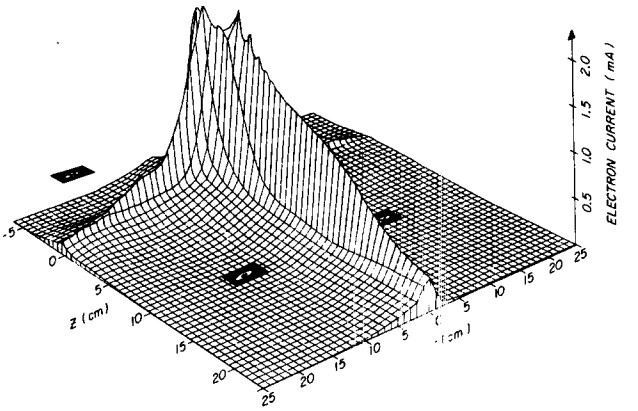

FIG. 2. Three-dimensional plot of electron-saturation current drawn by a 1.5 mm disk Langmuir probe as it was moved through the vertical plane containing the axis. The distance from the axis is r while z is the distance from the midplane. This plot was taken at a neutral pressure of 7.5×10^{-5} Torr and a magnetic field of 130 G in the center of the ring cusp and 210 G in the center of the point cusp.

The filament support could be inserted through either of the point cusps or through the ring cusp.

To produce a plasma, argon gas was admitted to the chamber with neutral pressures from $\sim3\times10^{-5}$ to $\sim1\times10^{-2}$ Torr. A current of 2–3 A was passed through each filament wire for heating, while the filaments were biased, typically at -60 V, with respect to the chamber. A discharge current of primary electrons (typically 0.3 A) flowed from the filaments, ionizing the argon gas to produce a plasma with typical densities of 10^{9}–10^{11} cm^{-3}. A narrow cathode sheath formed between the filaments and the bulk of the plasma, whose potential was within a few volts of ground. Electron temperatures ranged from 2 to 3 eV, while ion temperatures were a few tenths of an electron volt. The noise level in the ring and point cusps, as determined from fluctuations in the electron and ion saturation currents of a Langmuir probe circuit with a frequency response of up to 1 MHz, was $\delta n/n\approx2\%$–10%.

The major diagnostic used in this investigation was the Langmuir probe, typically a tantalum disk of 1.5 or 3 mm diameter. As a result of the limited spatial variation of the plasma potential and electron temperature, the relative electron, ion, and primary electron densities were determined by measuring the probe currents with the probe biased at $+9$, -90, and -9 V, respectively. Plasma potential measurements were made with an emissive probe constructed using a tungsten wire of 0.03 mm diameter and 0.5 cm length. The emissive probe was heated by the half-wave rectified output of a low-capacitance 6 V transformer whose input was controlled by a variac; the measurements were taken during the off cycle of the heating current.

III. EXPERIMENTAL RESULTS

We begin the presentation of the experimental results by showing, in Fig. 2, an overall three-dimensional perspective view of the relative electron density (i.e., electron-saturation current) throughout the cusp. A similar plot for the ions was also obtained. The escape of plasma through the ring and point cusps is evident, as is the confinement of the plasma to a neighborhood of the axis and the midplane (the symmetry plane midway between the coils).

Typical profiles of the electron, ion, and primary electron currents drawn by a Langmuir probe as it was moved across the ring cusp are shown in Fig. 3. These profiles may be interpreted as plots of relative density versus position. For the particular conditions of Fig. 3, the electron and ion leak widths (full width at half-maximum) were on the order of twice the hybrid gyrodiameter ($2r_h = 0.7$ cm) and the primary electron leak width was on the order of the primary gyrodiameter ($2r_p = 0.3$ cm). The relative density of primary electrons (n_p/n_e) decreased with increasing pressure and was about 5% in the center of the ring and point cusps at a neutral pressure of 7×10^{-5} Torr.

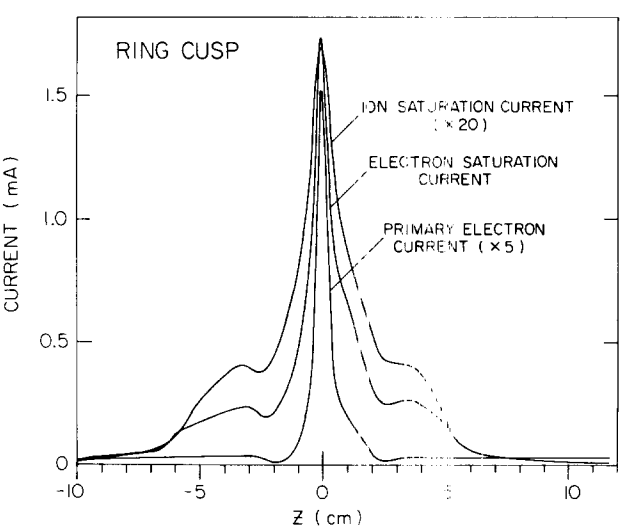

FIG. 3. Electron, ion, and primary electron current profiles taken with a 3 mm disk Langmuir probe moved across the ring cusp, at $r = 14$ cm. The neutral pressure was 5.5×10^{-5} Torr and the magnetic field was 110 G in the center of the ring cusp.

A. Quasineutrality

An important point that emerged from our investigations was that comparable electron and ion leak widths (as in Fig. 3) could only be attained at sufficiently high density. In Fig. 4, we present typical results from an investigation of the dependence of electron and ion leak widths on plasma density. The plasma density was varied, at fixed neutral pressure, magnetic field, and discharge voltage, by changing the filament temperature. The leak widths are plotted versus the dimensionless ratio of electron plasma frequency to electron gyrofrequency, $\omega_{pe}/\omega_{ce} \propto \sqrt{n_e}$, for fixed magnetic field. For $\omega_{pe}/\omega_{ce} < 0.1$, the electron and ion leak widths are very different, and the ion leak width is on the order of the ion gyrodiameter (5.2 cm). For $\omega_{pe}/\omega_{ce} > 0.5$, the ion and electron profiles are similar, consistent with quasineutrality ($n_e \approx n_i$). These data suggest the presence of electrostatic fields that inhibit cross-field motion of ions. While the density is varied by a factor of 10^4, the electron width broadens by only a factor of 2 while the ion leak width is reduced by more than a factor of 5, presumably as a result of electrostatic effects. In particular, for the quasineutral case, the electron and ion leak widths are nearly independent of density. In the remainder of our investigations, care was taken to ensure that the plasma density was sufficiently high so that the electron and ion density profiles have similar leak widths.

B. Leak widths

For neutral pressures in the 10^{-5} Torr range, the electron and ion leak widths were numerically on the order of a hybrid gyrodiameter. For pressures larger than $\sim 3\times 10^{-5}$ Torr, the leakage profiles tended to have "shoulders," i.e., regions in which the density remained nearly constant or increased slightly as the probe was moved away from the center of the cusp (see Fig. 3). These shoulders do not seem to be a result of the primary electrons, which are confined to a narrow channel on the order of their gyrodiameter. With increasing pressure, the width of the profile and height of the shoulders (relative to the peak height) both increased. The observation (discussed earlier) that the plasma density had little effect on the leak width when the plasma is quasineutral suggests that the increase in leak width with neutral pressure may be a result of diffusion caused by plasma–neutral collisions.

The pressure dependence of the ring cusp leak width d at fixed magnetic field and discharge current is shown in Fig. 5. [In Figs. 5, 6, and 7(b), m denotes the slope of the line.] The scaling $d \propto P^{1/2}$ was approximately obeyed as neutral pressure P was varied upward by a factor of 100 from the lowest pressure at which a discharge could be maintained. At sufficiently high pressures, the leak widths were nearly as large as the coil separation, and the escaping plasma was no longer constrained by the magnetic field but presumably by the mechanical constraint of the magnetic coils.

For fixed pressure and discharge current, the scaling of the ring cusp electron leak width with magnetic field is shown in Fig. 6. The ion leak widths exhibited similar behavior. The leak widths scaled as B^{-1} except for the case of very low pressure and high magnetic field, where the scaling $d \propto B^{-1/2}$ was approximately obeyed.

The electron and ion profiles in the point cusp generally showed a narrow central peak superimposed on a broader profile. The profiles of ion-saturation current for two pressures are shown in Fig. 7(a). The relative height of the broad profile increased with neutral pressure, while the width of the central peak remained nearly constant. Both widths descaling of the ion leak width with the magnetic field in the point cusp is shown in Fig. 7(b). The behavior of the electron leak width was similar. For pressures greater than 2×10^{-4} Torr, the leak width (full width at half-maximum) was primarily determined by the width of the broad profile and scaled approximately as $P^{1/2}B^{-1}$. The pressure scaling was not obeyed as well as it was in the ring cusp (the data were best fit with a $P^{0.7}$ dependence), presumably as a result of the sudden contribution of the broad profile to the leak

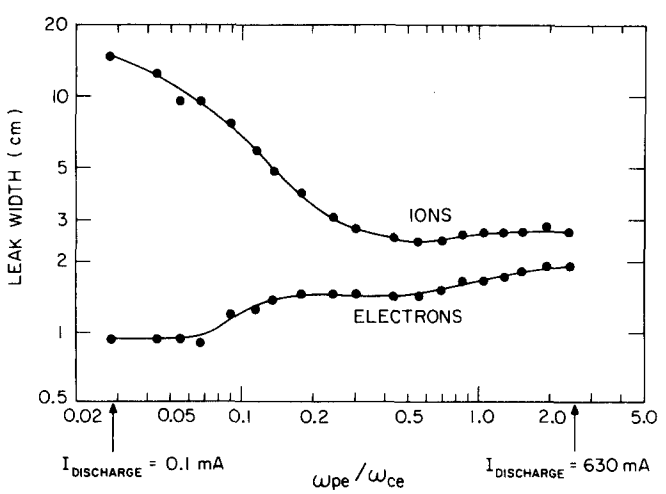

FIG. 4. Leak widths (full width at half-maximum) of electron and ion profiles in the ring cusp versus ω_{pe}/ω_{ce} as the plasma density was varied by changing the filament temperature with a neutral pressure of 7.1×10^{-5} Torr and a magnetic field of 110 G in the center of the ring cusp. The arrows indicate the discharge current for two values of ω_{pe}/ω_{ce}.

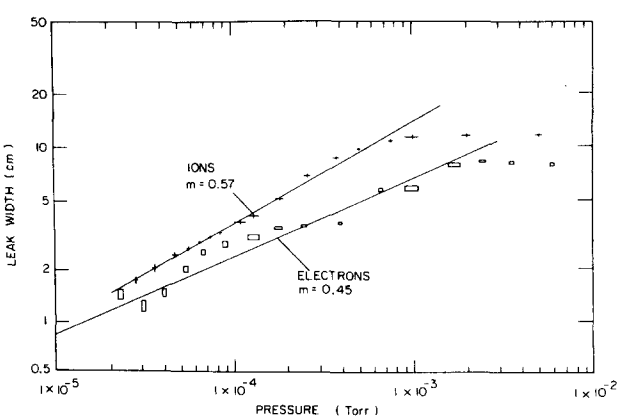

FIG. 5. Electron and ion leak widths in the ring cusp versus neutral pressure with a magnetic field of 110 G in the center of the ring cusp. (In this and the following similar figures, m denotes the slope of the lines.)

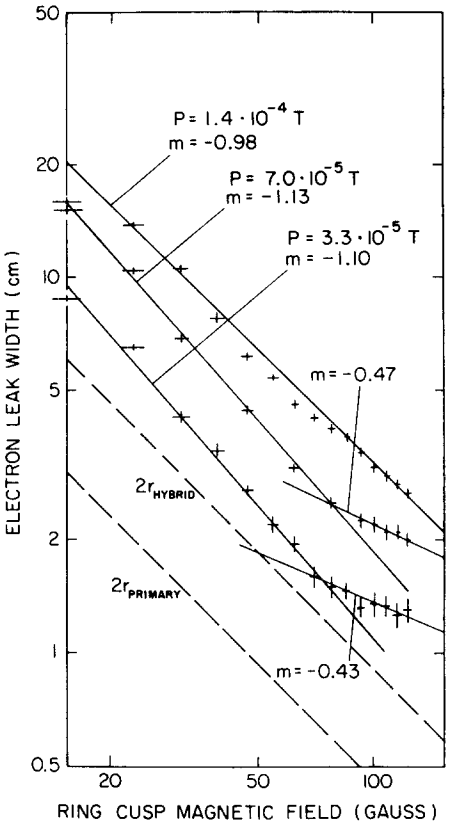

FIG. 6. Electron leak widths in the ring cusp versus magnetic field at three different neutral pressures. The hybrid gyrodiameter and primary electron gyrodiameter are also shown (dashed lines) for comparison.

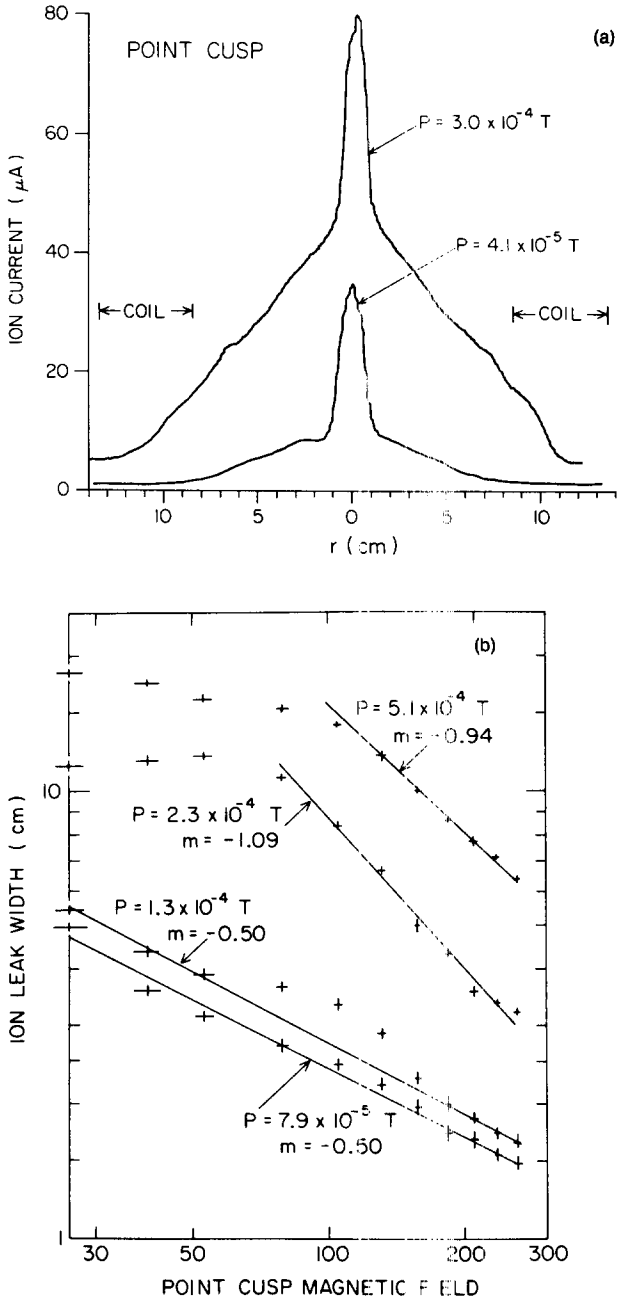

FIG. 7. Leak width measurements in the point cusp. (a) Ion-current profiles ($\propto$ ion density) taken with a 1.5 mm disk Langmuir probe at $z = 12$ cm with a magnetic field of 210 G in the center of the point cusp. (b) Ion leak widths versus magnetic field at four different neutral pressures.

width as its height exceeded one-half of the peak height. At sufficiently high pressures and low magnetic fields, the leak width was nearly as large as the coil inner diameter and the plasma was apparently constrained by the coil structure. At pressures below $\sim 1 \times 10^{-4}$ Torr, the leak width was nearly independent of neutral pressure and scaled as $B^{-1/2}$ over the full range of magnetic fields available.

The plasma leak widths and primary electron leak widths did not appear to be closely related. Although the plasma leak width broadened considerably with increasing pressure, the primary electron leak width was nearly equal to twice the primary gyrodiameter throughout the range of pressures and magnetic fields investigated. In addition, the plasma leak width changed by less than 10% when the primary electron energy was varied between 50 and 300 eV.

Measurements of electron and ion leak widths were also made with the filament support entering through the ring cusp. No substantial difference in behavior (or scaling) was observed with this configuration.

C. Electrostatic potentials

The potentials in the spindle cusp were determined using the emissive probe described earlier. The probe was heated to a temperature where the emitted current (with the probe biased below the plasma potential) was roughly equal to the collected current (with the probe biased above the plasma potential) in the center of the device. The potential of the inflection point ($d^2I/dV^2 = 0$) of the characteristic[18] agreed with the floating potential ($I = 0$) and was nearly independent of the probe temperature in a neighborhood of the temperature used. Thus the floating potential could be used as an indicator of the plasma potential.

The potential structures measured were similar to those previously reported.[11,12] Typical radial and axial potential profiles in the point cusp are shown in Fig. 8. There were potential troughs (with depths of 1–2 V and widths nearly equal to the particle leak width) in the center of the cusps

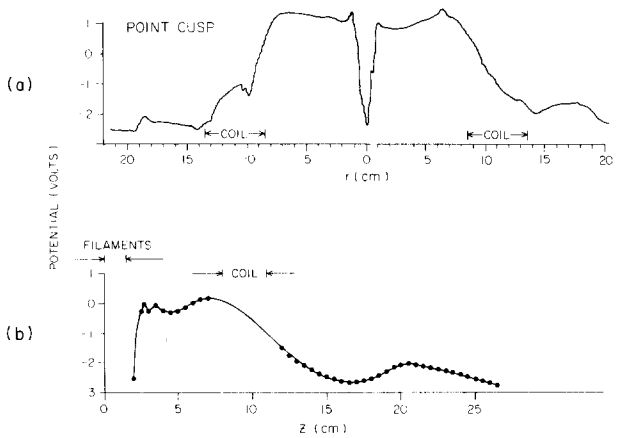

FIG. 8. Point cusp potential measurements. (a) Floating potential of an emissive probe moved *across the point cusp* (at $z = 12$ cm) with a neutral pressure of 1.0×10^{-4} Torr and a magnetic field of 210 G in the center of the point cusp. (b) Floating potential of an emissive probe moved *on axis* in the point cusp under the same conditions.

and positive "islands" near the coils [see Fig. 8(a)]. This potential structure is expected for cross-field ion confinement. In the ring cusp the trough was aligned with the midplane, while in the point cusp the trough was aligned with the axis. Figure 8(b) shows the variation with z of the potential at the bottom of the trough in the point cusp. The potential at the bottom of the trough was about two volts lower outside of the coils than in the center of the device, consistent with the acceleration of ions to a velocity of C_s as they flowed out of the cusp. The potential structures in the ring cusp were similar to those in the point cusp.

The average electric field strength in the trough was determined by dividing the depth of the trough by its width (full width at half-maximum). The electric field was determined in this way for a wide range of neutral pressure and magnetic field. In all cases, the electric field strength agreed within a factor of 2 with the value $2kT_e/ed$, where d was the leak width measured under the same conditions.

The electrostatic potentials were also investigated with the filament support in the ring cusp, again with no substantial change in behavior.

D. Flow velocities

The plasma flow velocities in the ring and point cusps were inferred from measurements of the propagation velocity of ion-acoustic waves. The propagation velocity of ion-acoustic waves in a plasma in which the ions are drifing is shifted by the ion flow velocity. By subtracting the ion-acoustic velocity C_s from the propagation velocity of ion-acoustic waves, the flow velocity can be determined.

Ion-acoustic waves were launched by applying a 20 V pulse of 4 μsec duration through a 6 μF capacitor to a grid located near the center of the device. For the ring cusp measurements, a cylindrical grid 8 cm in diameter, 4 cm in length, with a 3×3 mm mesh was placed around the filaments midway between the coils in an axially symmetric arrangement.

The disturbance launched from the grid was detected by observing the ion current to a collecting probe in the ring cusp. The disturbance consisted of a fast wave that reached the probe immediately, as well as a delayed pulse with $\delta n/n \approx 1\%$, which was interpreted as the ion-acoustic wave. The flow measurements were carried out at a neutral pressure of 1.5×10^{-4} Torr and a magnetic field strength in the middle of the ring cusp of 50 G. Under these conditions an ion-acoustic wave of sufficient amplitude could be observed throughout the cusp. A filter was used to improve the signal-to-noise ratio.

The time of arrival of the ion-acoustic wave relative to the launching time was determined for various probe positions in the midplane. The results of this investigation are shown in Fig. 9. Since the ion-acoustic velocity $C_s = (kT_e/m_i)^{1/2}$ is $2.4 \pm 0.2 \times 10^5$ cm/sec for $T_e = 2.5 \pm 0.5$ eV, these data show the acceleration in ion flow parallel to the magnetic field lines from a velocity of ~ 0.2 to $\sim 1.3\ C_s$.

A similar investigation was carried out in the point cusp, using a circular launching grid of 5 cm diameter and 1×1 mm mesh, which was placed between the filaments and the point cusp at a distance of 3 cm from the center of the filaments. Again, the pressure and magnetic field were chosen to optimize the wave launching and signal detection. At a neutral pressure of 2.4×10^{-4} Torr and a magnetic field in the center of the point cusp of 70 G, an acceleration in ion flow from a velocity ~ 0.1 to $\sim 1.1\ C_s$ was observed on axis in the point cusp, similar to the ring cusp behavior.

IV. DISCUSSION

A. Quasineutrality

At low plasma densities, the effects of plasma-generated electrostatic fields in the cusps will be negligible, so that the ion leak widths may be much larger than the electron leak widths. However, at sufficiently high densities, quasineu-

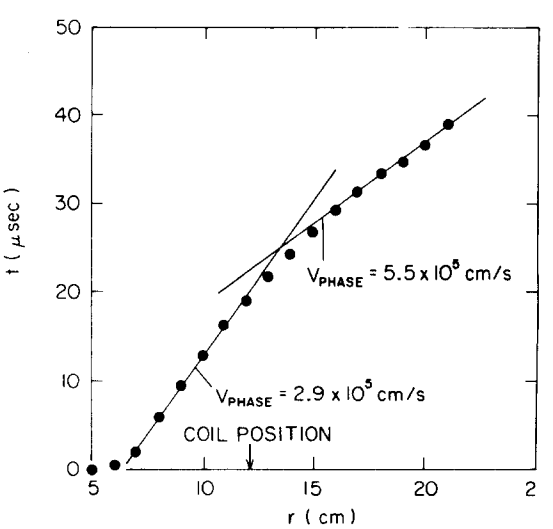

FIG. 9. Time of arrival of ion-acoustic wave launched into the ring cusp with a neutral pressure of 1.5×10^{-4} Torr and a magnetic field of 50 G in the center of the ring cusp.

trality must be attained so that similar electron and ion leak widths are obtained. The results of our investigations, as well as previous discharge experiments[7] and a numerical study,[19] indicate that quasineutrality is attained largely through the cross-field electrostatic confinement of ions. Our results, and the numerical studies by Clark,[19] suggest that the transition between non-neutral and quasineutral plasmas occurs when $\omega_{pe}/\omega_{ce} \approx 0.02 - 0.5$ in the cusp, and quasineutrality is satisfied for $\omega_{pe}/\omega_{ce} > 0.5$. These criteria may be understood in terms of a simple one-dimensional model.

We consider the low-density case in which the plasma is non-neutral, the self-consistent electrostatic fields are insignificant, and $n_e \gg n_i$ near the ring cusp midplane. Since the cross-field potential variations greatly exceed the variation along the field, we approximate $\nabla^2\phi \approx d^2\phi/dz^2$, where ϕ is the plasma space potential in the ring cusp. Then Poisson's equation near the ring cusp midplane for a plasma of full width d and an exponentially shaped profile $[n_e(z) = n_{e0} \exp(-2|z|/d)]$ is

$$\frac{d^2\phi}{dz^2} = 4\pi e n_{e0} \exp\left(-\frac{2|z|}{d}\right). \tag{1}$$

In order that the potential be symmetric about $z = 0$, we must have $d\phi/dz(0) = 0$. Setting $\phi(0) = 0$, we have

$$\phi(z) = 2\pi e n_{e0}\, d\{|z| + (d/2)[\exp(-2|z|/d) - 1]\}, \tag{2}$$

which gives

$$\phi(d/2) = 0.4\,\pi e n_{e0} d^2. \tag{3}$$

This result is not very sensitive to the electron profile shape; for example, with a flat-top electron distribution we obtain $\phi(d/2) = 0.5\pi\, e n_{e0} d^2$.

When $\phi(d/2) \gtrsim kT_i/e$, the assumption that self-consistent electrostatic fields are insignificant breaks down, since a potential trough of this depth can confine thermal ions. Thus we expect that the plasma has partially attained quasineutrality when the electron density is sufficiently large so that $\phi(d/2) = kT_i/e$, which is equivalent to

$$d/\lambda_{D_e} = (10T_i/T_e)^{1/2}, \tag{4}$$

where λ_{D_e} is the electron Debye length in the center of the cusp. Equation (4) corresponds to the standard criterion that the Debye length must be smaller than the plasma density scale length in order to have quasineutrality. Writing $d/\lambda_{D_e} = (d/r_{ce})(r_{ce}/\lambda_{D_e})$, and noting that $r_{ce}/\lambda_{D_e} = \omega_{pe}/\omega_{ce}$, we can write Eq. (4) as

$$\omega_{pe}/\omega_{ce} = (r_{ce}/d)(10T_i/T_e)^{1/2}. \tag{5}$$

For the conditions under which that data of Fig. 4 were obtained, $T_e = 2$ eV, $T_i = 0.2$ eV, $B = 110$ G, and $r_{ce} = 0.03$ cm, so that $d/r_{ce} = 33$. Equation (5) then predicts a transition to quasineutrality when $\omega_{pe}/\omega_{ce} = 0.03$, in agreement with the data. The predictions of this analytical model are also in good agreement with the numerical results of Clark.[19] The success of this model supports the interpretation of Fig. 4 as the attainment of quasineutrality and cross-field confinement of ions as a result of electrostatic effects.

B. Leak widths

The observed leak widths may be understood in terms of a model in which plasma escapes from the cusp at the ion-acoustic speed while diffusing across the magnetic field.[4] In this model (discussed further in Appendix A), the leak width is

$$d = (2\bar{D}R/C_s)^{1/2}, \tag{6}$$

where $\bar{D}$ is the effective diffusion coefficient and R is the coil radius. In general, the diffusion coefficient will be determined by neutral particle collisions (i.e., classical diffusion) and nonclassical diffusion (e.g., Bohm diffusion) and if we assume that these processes are linearly additive, we may write

$$D = D_c + D_B = \left(\frac{r_{ce}^2}{\tau_c}\right)\left(1 + \frac{T_i}{T_e}\right) + \frac{ckT_e}{16eB}, \tag{7}$$

where D_c and D_B are the classical and Bohm diffusion coefficients and τ_c is the electron–neutral collision time.[20] At sufficiently high pressures and low magnetic fields, classical diffusion dominates and Eq. (6) predicts a leak width

$$d = \left[\frac{2R}{C_s}\left(\frac{r_{ce}^2}{\tau_c}\right)\left(1 + \frac{T_i}{T_e}\right)\right]^{1/2} \propto m_i^{1/4}(\sigma T_e)^{1/2} P^{1/2} B^{-1}, \tag{8}$$

for $T_i \ll T_e$, where σ is the electron–neutral collision cross section.

The scaling with neutral pressure and magnetic field given by this expression agrees with the observed scaling for sufficiently high neutral pressure and low magnetic field. The dependence upon ion mass and magnetic field predicted by this equation has been previously observed[7] and is identical to the scaling of the hybrid gyroradius. Equation (8) predicts a leak width approximately equal to a hybrid gyroradius for the typical electron temperatures and neutral pressure of the discharge. Numerically, the result of Eq. (8) (in which the effective diffusion coefficient is calculated at a point midway between the cusp and the filaments, where $B \approx B_{cusp}/2$) agrees within a factor of 3 with the result of this experiment and those of Ref. 7. This is a reasonable agreement in light of the approximations used to obtain Eq. (6).

Recently, Koch and Matthieussent[15] have proposed that the leak width of a collisional cusp may be evaluated by assuming that plasma diffuses across the magnetic field only when the perpendicular diffusion coefficient of electrons exceeds that of ions, i.e., when $r_{ce}r_{ci}/\lambda_e\lambda_i > T_e/T_i$, where λ_e and λ_i are the electron and ion mean free paths. For $T_e = 2$ eV, $T_i = 0.2$ eV, and neutral pressures less than 10^{-3} Torr, this will be satisfied only when $B < 1$ G. For the range of magnetic fields of our device, this occurs only within $\frac{1}{2}$ cm of the center of the chamber, inside of the filament structure. As a result, this model neglects cross-field diffusion outside of the plasma production region (the region occupied by primary electrons) and cannot account for the observation of plasma profiles that were much broader than the primary electron profile. However, this model may prove more useful in multidipole and picket-fence geometries, with their relatively large field-free regions.

The importance of collisions in a plasma of scale length 10 cm with a neutral pressure of 10^{-4} Torr is somewhat counterintuitive, since the mean free path for electron–neutral collisions is ~ 3 m. However, quasineutrality requires that the electrons tend to escape at the ion-acoustic speed. In a time R/C_s, a typical thermal electron will travel 30 m, suffer (on average) ten collisions, and diffuse across the magnetic field a distance $(10)^{1/2} r_{ce}$, in agreement with the results of Eq. (8).

The breakdown of the $P^{1/2}B^{-1}$ scaling at high magnetic field and low neutral pressure suggests that neutral particle collisions are no longer the dominant factor in determining the leak width. Under the assumption that Bohm diffusion dominates classical diffusion, Eq. (6) predicts

$$d = [(2R/C_s)(ckT_e/16eB)]^{1/2} \propto m_i^{1/4} T_e^{1/4} B^{-1/2}, \tag{9}$$

for $T_i \ll T_e$. This expression agrees with the observed scaling with the magnetic field in the low neutral pressure, high-magnetic field case, for which $D_B > D_c$ is expected. The numerical value of the leak width calculated from this expression agrees with the observed leak width within a factor of 3, again a reasonable agreement in light of the approximations used to obtain Eq. (6).

C. Electrostatic potentials

The electrostatic potential measurements indicated the formation of negative troughs in the cusps, aligned along the magnetic field. The potential in the troughs decreases in the direction of plasma flow. The observations are in agreement with the self-consistent potentials expected in order to maintain quasineutrality. The electric fields parallel to **B** prevent the rapid escape of electrons while those perpendicular to **B** provide cross-field confinement of ions.

As a result of the high mobility of electrons along field lines, we may expect a Boltzmann distribution of electron density along a given field line. This implies that the plasma potential along a field line must decrease in the direction of decreasing density, i.e., the direction of flow. The potential data of Fig. 8 show that the potential along the field line in the center of the point cusp indeed decreases in the direction of flow by about T_e, while the density (Fig. 2) decreases by about a factor of 3, in agreement with the behavior of a Boltzmann electron distribution.

The ions in the cusp are moving at the ion-acoustic velocity and thus have a kinetic energy on the order of $kT_e/2$. In order to confine these ions in a trough of width d, the potential must rise by about $kT_e/2e$ within a distance $d/2$ of the center of the trough, giving rise to a perpendicular electric field of order kT_e/ed. The data of Fig. 8, as well as the data taken throughout a wide range of neutral pressure and magnetic fields, show that the perpendicular electric fields are indeed of this order of magnitude.

Thus the observed electrostatic potentials are in reasonable qualitative and quantitative agreement with the self-consistent potentials expected in order to maintain quasineutrality, thus providing cross-field confinement of the ions.

D. Flow velocities

The density profile of Fig. 2 shows that the plasma leak width in the cusps is smallest where the magnetic field is greatest, suggesting that the plasma flow follows the magnetic field lines, converging inside of the magnet coils and diverging outside of the coils. In addition, the density decreases in the direction of plasma flow. Under these circumstances, the steady-state flow of a quasineutral plasma with a scalar pressure may be described as a "magnetic" Laval nozzle (see Appendix B). This model predicts the acceleration of ions to a supersonic velocity as they pass through the cusps, a phenomenon that has been previously observed in a Q machine in a magnetic mirror configuration.[21] Our measurements show that supersonic flow is achieved in the cusps, in agreement with this model.

V. SUMMARY AND CONCLUSIONS

The major results and conclusions of this investigation may be summarized in the following points.

(a) For $\omega_{pe}/\omega_{ce} > 0.5$ (i.e., $\lambda_{D_e} \ll d$), self-consistent electrostatic fields result in cross-field confinement of ions.

(b) For sufficiently high neutral pressures and low magnetic fields, the leak width scales as $P^{1/2} B^{-1}$, while at low neutral pressures and high magnetic fields it scales as $P^0 B^{-1/2}$. These scalings are consistent with a model in which plasma diffuses across the magnetic field as a result of the combined effects of neutral-plasma collisions and noncollisional Bohm diffusion.

(c) The measured electrostatic potentials are in reasonable agreement with the self-consistent potentials expected to maintain quasineutrality, inhibiting the flow of electrons parallel to **B** and the flow of ions perpendicular to **B**.

(d) Ions flowing through the cusps are accelerated to the ion-acoustic velocity, in agreement with the expected flow of plasma in a "magnetic" Laval nozzle.

ACKNOWLEDGMENTS

We wish to thank S. Cartier, N. D'Angelo, G. Knorr, and K. Clark for useful discussions, and A. Scheller for technical assistance.

This work was supported in part by the Office of Naval Research and by a Graduate College Block Grant from the University of Iowa.

APPENDIX A: LEAK WIDTH SCALING

In this Appendix, we present a derivation of Eq. (6) for the leak width. The main assumptions of this steady-state model are (1) cross-field flow is a result of diffusion (and possibly drifts around the axis); (2) plasma production is localized in the vicinity of the axis and the midplane; and (3) the plasma in the cusps is flowing outward at approximately the ion-acoustic speed.

The second assumption is supported by measurements of the primary electron density, which show that they are localized within a primary electron gyrodiameter of the axis and midplane. The third assumption follows from the flow velocity measurements.

We begin with a derivation of the diffusion equation

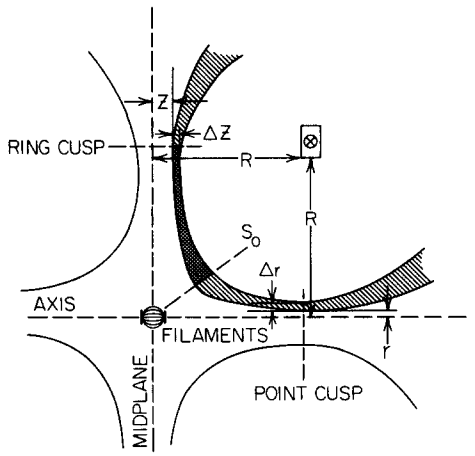

FIG. 10. Schematic for the model of plasma diffusion and flow in the ring and point cusps.

appropriate for the ring cusp. Consider the plasma flow in the flux tube represented by the shaded region of Fig. 10. This flux tube is a volume of revolution (about the axis) bounded by magnetic field lines whose distances from the midplane are z and $z+\Delta z$, with $\Delta z \ll z$. Since the component of flow velocity along the magnetic field is oppositely directed in the ring and point cusps, there is a surface S_0 consisting of points at which this component of velocity vanishes. By assumption (2), the particle flux $\mathbf{J}$ obeys $\nabla \cdot \mathbf{J} = 0$. Integrating this relation over the portion of the shaded region between the surface S_0 and the ring cusp gives

$$0 = \int_V \nabla \cdot \mathbf{J}\, dV = \int_S \mathbf{J} \cdot d\mathbf{A}$$
$$= I_\perp(z+\Delta z) - I_\perp(z) + n(z) C_s (2\pi R\, \Delta z), \quad \text{(A1)}$$

where $I_\perp(z)$ and $I_\perp(z+\Delta z)$ are particle currents perpendicular to B through the inner and outer surfaces bounding V, R is the coil radius, and $n(z)$ is the density in the cusp. Dividing by Δz and taking the limit $\Delta z \to 0$ yields

$$n(z) C_s (2\pi R) = -\frac{dI_\perp(z)}{dz}. \quad \text{(A2)}$$

The term $I_\perp(z)$ can be written as

$$I_\perp(z) = \int_{S_z} \mathbf{J} \cdot d\mathbf{A} = -\int_{S_z} D_\perp \nabla n \cdot d\mathbf{A} = -\langle D_\perp (\nabla n)_\perp \rangle A, \quad \text{(A3)}$$

where $D_\perp$ is the diffusion coefficient and A is the area of the inner surface S_z of the shaded region. Approximating A by πR^2 and introducing the effective diffusion coefficient $\bar{D}(z) = \langle D_\perp (\nabla n)_\perp \rangle / [dn(z)/dz]$ yields

$$I_\perp(z) = -\bar{D}(z) \frac{dn(z)}{dz} (\pi R^2). \quad \text{(A4)}$$

When $\bar{D}(z)$ is independent of z, Eqs. (A2) and (A4) imply

$$\frac{d^2 n}{dz^2} = \frac{2C_s}{\bar{D}R} n(z), \quad \text{(A5)}$$

for $z \neq 0$. With boundary conditions $n(\pm\infty) = 0$, Eq. (A5) has the solution

$$n(z) = n_0 \exp[-|z|/(\bar{D}R/2C_s)^{1/2}], \quad \text{(A6)}$$

with leak width

$$d = 2(\bar{D}R/2C_s)^{1/2} = (2\bar{D}R/C_s)^{1/2}. \quad \text{(A7)}$$

A similar analysis may be applied to the point cusp using the coordinate r in place of z. In place of Eq. (A2) we have

$$n(r) C_s (2\pi r) = -\frac{dI_\perp(r)}{dr}. \quad \text{(A8)}$$

We now approximate $I_\perp(r)$ as

$$I_\perp(r) \approx -\bar{D} \frac{dn(r)}{dr} (2\pi r R). \quad \text{(A9)}$$

Eliminating $I_\perp(r)$ from Eqs. (A8) and (A9) and assuming that $\bar{D}$ is independent of r yields

$$\frac{d^2 n}{dr^2} + \frac{1}{r}\frac{dn}{dr} - \left(\frac{C_s}{R\bar{D}}\right) n = 0, \quad \text{(A10)}$$

which is the modified Bessel equation, with solution

$$n(r) = n_0 K_0(r/d), \quad \text{(A11)}$$

where $d = (\bar{D}R/C_s)^{1/2}$. For $r/d > 0.2$, the approximation

$$K_0(r/d) \approx (\pi d/2r)^{1/2} \exp(-r/d)$$

is accurate within 25%, indicating that the scale length of the leak width is $d/2 = (\bar{D}R/C_s)^{1/2}$.

APPENDIX B: THE "MAGNETIC" LAVAL NOZZLE

We consider the steady-state flow of a quasineutral plasma with a scalar pressure. In accordance with our observations, we describe the case of converging–diverging flow in the cusps in which the plasma density decreases in the direction of flow. We begin with the momentum equations of the ions and electrons:

$$m_i n (\mathbf{v} \cdot \nabla)\mathbf{v} = en\left(\mathbf{E} + \frac{\mathbf{v} \times \mathbf{B}}{c}\right) - \nabla P_i,$$
$$m_e n (\mathbf{v}_e \cdot \nabla)\mathbf{v}_e = -en\left(\mathbf{E} + \frac{\mathbf{v}_e \times \mathbf{B}}{c}\right) - \nabla P_e. \quad \text{(B1)}$$

Adding these equations, neglecting the electron mass term, and taking the scalar product with the ion velocity $\mathbf{v}$ gives

$$m_i n v (\mathbf{v} \cdot \nabla) v = -(\mathbf{v} \cdot \nabla) P - en\left(\frac{\mathbf{v}_e \times \mathbf{B}}{c}\right) \cdot \mathbf{v}, \quad \text{(B2)}$$

where $P = P_e + P_i$ is the total pressure. The electron and ion flow velocities in the cusps consist mainly of flow along the magnetic field (and possibly drifts around the axis), so we can neglect the last term in Eq. (B2). Since the density n is monotonically decreasing in the direction of flow, we can consider the pressure on a given flow as a function of n, thus obtaining

$$v(\mathbf{v} \cdot \nabla) v = \frac{-1}{nm_i} \mathbf{v} \cdot \nabla P = \frac{-1}{n}\left(\frac{1}{m_i}\frac{dP}{dn}\right) \mathbf{v} \cdot \nabla n$$
$$= \frac{-1}{n} C_s^2\, \mathbf{v} \cdot \nabla n, \quad \text{(B3)}$$

where $C_s^2 = 1/m_i\, dP/dn$.

If we consider a small tube around a given line of flow whose surface consists of neighboring lines of flow and whose cross-sectional area is A, the ion-continuity equation can be written as

$$0 = \lim_{A\to 0}\left(\frac{(\mathbf{v}\cdot\nabla)(nvA)}{nvA}\right)$$

$$= \frac{\mathbf{v}\cdot\nabla n}{n} + \frac{\mathbf{v}\cdot\nabla v}{v} + \lim_{A\to 0}\frac{\mathbf{v}\cdot\nabla A}{A}, \tag{B4}$$

where the limit is taken over a sequence of tubes contracting nicely to the given line of flow. Eliminating the density from Eqs. (B3) and (B4) yields

$$(M^2 - 1)\frac{(\mathbf{v}\cdot\nabla)v}{v} = \lim_{A\to 0}\frac{(\mathbf{v}\cdot\nabla)A}{A}, \tag{B5}$$

where $M = v/C_s$ is the Mach number. Since $\mathbf{v}\cdot\nabla n < 0$, Eq. (B3) implies that $\mathbf{v}\cdot\nabla v > 0$. Equation (B5) indicates that this steady increase in velocity is possible only if $M < 1$ in regions of converging flow ($\lim \mathbf{v}\cdot\nabla A/A < 0$) and $M > 1$ in regions of diverging flow ($\lim \mathbf{v}\cdot\nabla A/A > 0$). Thus, for the converging–diverging flow in a cusp, the ions must be accelerated from a subsonic to a supersonic velocity as they flow out of the cusp.

[1]R. Limpaecher and K. R. MacKenzie, Rev. Sci. Instrum. **44**, 726 (1973).
[2]R. J. Taylor, K. R. MacKenzie, and H. Ikezi, Rev. Sci. Instrum. **43**, 1675 (1972).
[3]M. G. Haines, Nucl. Fusion **17**, 811 (1977).
[4]I. Spalding, in *Advances in Plasma Physics*, edited by A. Simon and W. B. Thompson (Interscience, New York, 1971), Vol. 4, p. 79.
[5]See, for example, K. N. Leung, R. D. Collier, L. B. Marshall, T. N. Gallaher, W. H. Ingham, R. E. Kribel, and G. R. Taylor, Rev. Sci. Instrum. **49**, 321 (1978).
[6]T. E. Wicker and T. D. Mantei, J. Appl. Phys. **57**, 1638 (1985).
[7]N. Hershkowitz, K. N. Leung, and T. Romesser, Phys. Rev. Lett. **35**, 277 (1975); K. N. Leung, N. Hershkowitz, and K. R. MacKenzie, Phys. Fluids **19**, 1045 (1976).
[8]R. Jones, Nuovo Cimento **34**, 157 (1982).
[9]H. Kozima, S. Kawamoto, and K. Yamagiwa, Phys. Lett. **86**, 373 (1981).
[10]R. Jones, Plasma Phys. **21**, 505 (1979).
[11]S. Cartier, Master's thesis, University of Iowa, 1980.
[12]N. Hershkowitz, J. R. Smith, and J. R. DeKock, Plasma Phys. **21**, 823 (1979); N. Hershkowitz, J. R. Smith, and H. Kozima, Phys. Fluids **22**, 122 (1979).
[13]I. S. Landman and F. R. Ulinich, Sov. J. Phys. **8**, 371 (1982).
[14]G. Knorr and D. Willis, Z. Naturforsch. **37a**, 780 (1982).
[15]C. Koch and G. Matthieussent, Phys. Fluids **26**, 545 (1983).
[16]G. Knorr and R. Merlino, Plasma Phys. Controlled Fusion **26**, 433 (1984).
[17]R. Yoshino and T. Sekiguchi, J. Phys. Soc. Jpn. **44**, 1969 (1978).
[18]J. R. Smith, N. Hershkowitz, and P. Coakley, Rev. Sci. Instrum. **50**, 210 (1979).
[19]K. L. Clark, Master's thesis, University of Iowa, 1984.
[20]N. A. Krall and A. W. Trivelpiece, *Principles of Plasma Physics* (McGraw-Hill, New York, 1973), p. 333.
[21]S. A. Andersen, V. O. Jensen, P. Nielsen, and N. D'Angelo, Phys. Fluids **12**, 557 (1969).